Flow and turbulence characterization as an onset for assessing the stability of gravel beds

D. Duma, S. Erpicum, P. Archambeau, M. Pirotton & B. Dewals
University of Liege (ULg), Hydraulics in Environmental and Civil Engineering (HECE), Liege, Belgium. Email: diana.duma@ulg.ac.be

ABSTRACT: The flow characteristics, such as velocity profiles and turbulence intensities, are of high practical relevance in the assessment of riverbed stability. So far, the Shields diagram remains the most widely accepted approach for defining the initiation of sediment motion. However, it faces a number of shortcomings. In principle, it is only valid for uniform flow conditions and, under non-uniform flow conditions, it fails to account properly for the influence of turbulence in sediment entrainment. In this paper, we focus on a more detailed description of quasi-uniform and non-uniform flow characteristics in the vicinity of the critical flow conditions for inception of motion of gravel beds. Laboratory experiments were designed, involving two configurations. First, the entire bottom of the flume was paved with stones of uniform diameter (8 or 15 mm), leading to quasi-uniform flow conditions. Second, the flume bottom was smooth upstream of the zone of measurement while the downstream part was covered with gravels, leading to a sudden smooth-to-rough transition. The flow velocity was obtained by acoustic measurements and the turbulence intensity was calculated for both configurations. By fitting the velocity profile to a modified logarithmic law, the shear velocity was estimated. Standard approaches for predicting the threshold of motion, initially developed for uniform flows, were compared to other methods, based on depth-averaged turbulence kinetic energy, recently proposed in literature for non-uniform flow conditions.

1. INTRODUCTION

Successful and cost-effective design of riverbed protections against erosion requires a deep understanding of the complex interactions between turbulent flow forces and forces stabilizing the riverbed. Although much research has been accumulated, our knowledge is still far from being mature and reliable for practical applications. Whether naturally armoured or protected by engineering works, the riverbed superficial layer is usually made of stones, large enough to withstand the hydraulic loads in a range of flow conditions. The size of these stones may even be of the same order of magnitude as the water depth. The entrainment of stones in rivers exhibits an intermittent behavior, in which near-bed turbulence plays a major part. Stones often get moved as a result of bursting flow motions (ejections and sweeps). However, most of the existing approaches for assessing stones stability are based on the bed shear stress, which truly reflects the turbulent characteristics of the flow only in the case of uniform flows (Nezu and Kyōto 1977, Yalin 1977). Indeed, all standard bed stability equations were developed for uniform flow conditions (Shields 1936). Consequently, no physical relationship between flow forces and bed damage is available for general non-uniform flow conditions, although these are the flow conditions of highest practical relevance as they prevail downstream of most hydraulic structures

For assessing the stability of stones under a fluid flow, the most widely used conceptual framework so far relies on the stability threshold concept. But the threshold conditions are very difficult to establish unequivocally (Buffington and Montgomery 1997) and strongly depends on the grain size distribution (Yalin 1977). Also, a clear-cut definition of the exact moment when stones start to move is impossible, due to the stochastic nature of particles entrainment and the intermittent behavior of sediment transport (Yalin 1977, Hoffmans 2012). As a result, different inconsistent definitions of the inception of sediment motion have been used in literature, usually based on subjective observations such as “occasional and local particle movement” or “particle movement at several locations”.

Solving this issue theoretically remains particularly intricate, due to the complexity of interactions between flow and sediments. Also, very detailed numerical simulations at the grain-scale could provide promising results, but their computational cost remains very high. Runtimes of the order of months are reported in literature (Fukuoka 2013). Moreover, such numerical simulations of flow over rough surfaces rely on simplifying assumptions to reduce the computational cost, such as the velocity profile following a semi-logarithmic law near the wall (Jeffcoate et al. 2012). These assumptions, as well as other modeling features, may induce significant errors (Dwivedi et al. 2012, Cataño-Lopera et al. 2013).

In the last decade, experimental researchers developed a totally different approach, which quantifies the flow forces by means of a new set of parameters combining explicitly the velocity and turbulence distributions over a certain water depth above the riverbed, while remaining reasonably accessible for engineering applications (Jongeling et al. 2003, Hofland 2005, Hoan 2008, Hoffmans 2012). So far only two of these formulas were linked to a quantitative and clearly defined measure of stone motion (Hofland 2005, Hoan 2008). This approach is referred to as the stone transport concept, in which the threshold is replaced by a mobility parameter, estimated as a function of a stability parameter used to quantify the flow forces. These contributions pave the way for the development of more generic, physically-based, and continuous cause-and-effect relationships between the hydraulic loads (including turbulence) and the bed response. Nonetheless, there is still a need for more experimental verifications, supported by high quality turbulence measurements.

This paper brings new experimental data, which are analyzed using the stone transport conceptual frame work. The turbulent kinetic energy profiles of the flow are linked to the inception of motion of coarse sediments thanks to the experimental measurements obtained with an ultrasound velocity profiler (UVP) transducer. These tests highlight the overwhelming influence of turbulence on the stone movement.

2. EXPERIMENTAL CONFIGURATION

The experiments were conducted in a horizontal flume 6 m long and 15 cm wide, using uniform sediments of 8 mm, respectively 15 mm, representing an armor layer for riverbed protection. The aim of these tests was to highlight the influence of turbulence on the bed damage. Thus, two configurations of the flume bottom were considered (figure 1): the entire bottom of the flume was paved with stones (configuration 1) or the bed was smooth upstream of the measurement area (configuration 2). In each test series, the procedure followed two steps for each considered discharge: i) the stones were laid on the bottom of the flume and for 2 h the number of entrained stones was recorded; ii) the stones were glued on the flume bottom and flow velocity was measured with a UVP probe over a window of 200 mm, for the same hydraulic conditions as in step 1.

The discharge was measured with a flowmeter and increased by steps of about 0.5 l/s from one test to another. The covered range of mean flow velocity was from 700 mm/s up to 830 mm/s. In each test, measurements were started after a few minutes, enabling the flow to become steady. The water level was measured in 6 points along the flume, with ultrasonic sensors placed every meter. Since these sensors are sensible to atmospheric temperature, a recalibration was necessary before each test.

a)

b)

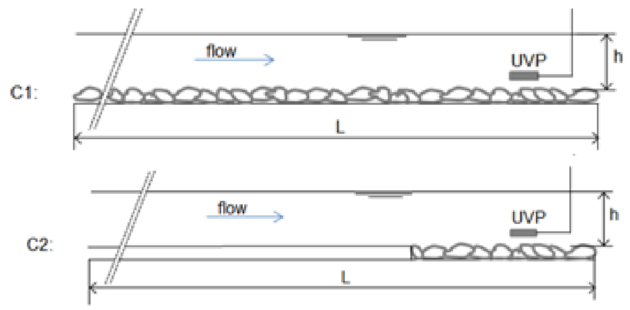

Figure 1. Geometric configurations. Lateral view.
a) configuration no. 1 (rough bottom); b) configuration no. 2 (smooth to rough transition)

3. ULTRASOUND VELOCITY PROFILER (UVP)

The UVP is a device for measuring an instantaneous velocity profile in liquid flow along the ultrasonic beam axis by detecting the Doppler shift frequency of echoed ultrasound as a function of time (Met-Flow 2000).

In this research, 1 MHz UVP probes, 40 mm length and 16 mm in diameter were used to measure instantaneous velocities in a recirculating hydraulic flume. Different sampling frequencies were tested to identify the optimal trade-off between the measurement depth and the accuracy of the results. The maximum depth of the measurement window was varied between 165 mm and 430 mm, with a sampling distance of 3 mm in which the instantaneous velocity is recorded. The sampling rate is directly linked to the depth of the measurement window through the following relationship: $f_s = \frac{c}{2 n_{rep} s_{max}}$, where f_s is the sampling rate [Hz], c is the sound velocity in water [m/s], n_{rep}= 32 is the number of pulse repetitions [-] and s_{max} is the depth of the measurement window [m]. A higher sampling rate provides more accurate results, but a smaller measurable depth. Based on a number of tests performed in the same hydraulic conditions, but with different sampling rate between 38 Hz and 127 Hz, f_s =100 Hz was selected as the sampling rates achieving a satisfactory accuracy.

These measurements were carried out close to the surface, but also close to the rough bed where the velocity fluctuations are high.

The power spectral density (PSD) was used to represent the distribution of energy in the measured velocity signal as a function of the frequency. PSD shows the relative strength of fluctuations at different scales. The spectrum was computed by taking the fast Fourier transform (FFT) of the recorded velocity time series.

As UVP probes fail to provide accurate results, a preliminary test was undertaken to analyze the influence on the results of injecting small hydrogen bubbles in the flow. Average velocity, shear velocity and turbulent kinetic energy were compared and the results revealed a weak influence at hydrogen bubbles in the present case. The spectral analysis also showed no significant effect of the presence of hydrogen bubbles. Therefore, hydrogen was not infected in subsequent tests.

4. EXPERIMENTAL RESULTS

The optimal length of the time series was defined based on preliminary tests. About 80 series of 60,000 samples were recorded and processed. Half of them were measured near the bed and the other half near the free surface. They were considered as reference series. Next, each of them was divided into sub-series of 10,000 to 30,000 values. The mean velocity and turbulence kinetic energy were estimated for each sub-series. By comparing these values with those computed from the reference series, the subseries of 20,000 samples were chosen for all following tests, due to their relative error which does not exceed $\pm$3% regarding the turbulent kinetic energy and $\pm$ 0.5% for the estimation of the mean velocity.

The ultrasound waves may get reflected or deflected in a wrong direction, when the flow velocity exceeds the preset velocity range of the device or when there are interactions with previous pulses reflected on the boundaries of complex geometries (stones in the bed). The lack of reflecting particles or a week signal can also introduce a wrong value (spikes) in the recorded data. In order to process the recorded data, two steps were necessary: detecting the spikes and replacing them. This was achieved using Goring's algorithm (Goring and Nikora 2002).

4.1. Velocity

The UVP transducer was placed downstream of the considered measurement window. A local disturbance of the flow induced by the transducer along the X-axis was observed, so that all considered measurements were taken at a distance of minimum 8 cm upstream of the probe. Instantaneous velocities were recorded over a length of 100 mm, in the main direction of the flow and in 10-12 points on the flow depth. The range of recorded values is in-between 0 and 1.5 m/s. As the UVP probe records data from a sample of 2.96 mm along the main flow axis, velocity profiles in over 30 cross-sections were obtained. Averages over 3 mm, 10 mm, 50 mm and 100 mm along the flow axis (x-axis) were analyzed. In all tests, no matter the configuration nor the stones diameter, the variation in the velocity profile along the stream direction was low, particularly in the lowest part of profile (figure 2). Therefore, an averaged value over 100 mm was considered in all subsequent analyses.

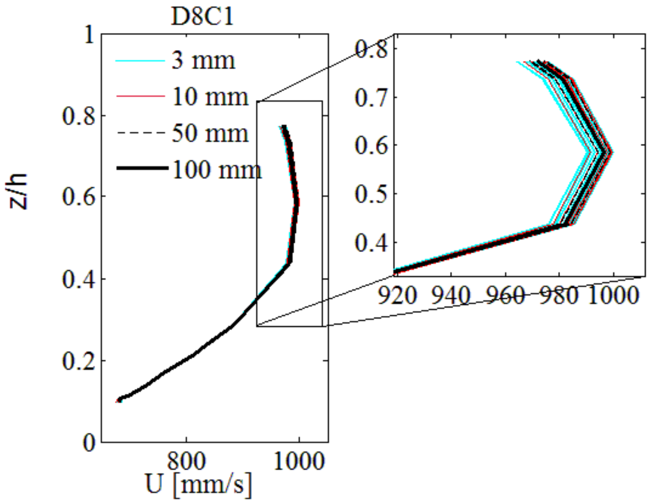

Figure 2. Velocity profile over a rough bed, (d=8 mm), for a discharge of 15 l/s. Averages over 3 mm, 10 mm, 50 mm and 100 mm along the main flow direction.

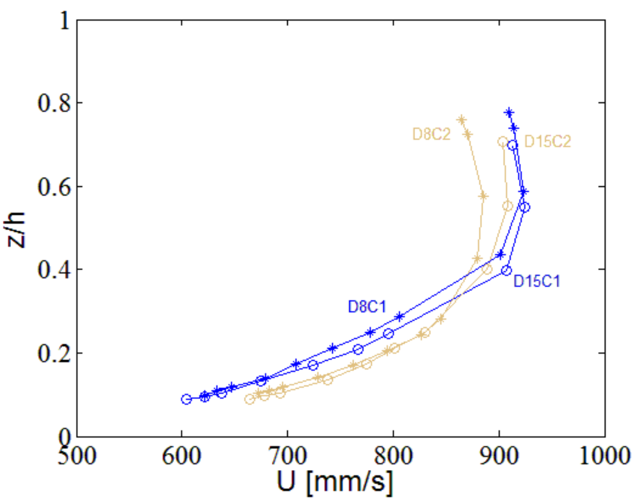

Figure 3. Velocity profile over a rough bed, respectively over a smooth-to-rough transition, (d=8 mm and d=15 mm), for a discharge of 15 l/s.

Figure 3 reveals a slight difference between the mean velocity profiles in the two configurations. The near-bed slope of the profile in the first configuration is smaller than in the second configuration. This observation is consistent with the development of a higher bed shear stress when the upstream part of the flume bottom is covered with gravels (configuration 1).

4.2. Shear Velocity

Shear velocity u_* is an important parameter in geophysical flows, in particular with respect to sediment transport dynamics. Here two methods are used to obtain the shear velocity of the flow. First, a friction law was used in a backwater curve computation and the computed water surface profiles were compared with the measured ones in the first configuration. Second, a logarithmic law was fit to the velocity profile in the main stream direction, for both configurations.

Using backwater profile computations in configuration 1, the roughness of the bottom and the walls of the flume were estimated by comparing measured and computed water levels. The friction formula of Barr-Bathurst was used (Machiels et al. 2011). To determine the roughness height of the walls a first series of tests was conducted without stones on the bottom (smooth PVC bed). Although some discrepancies remained between measured and computed water profiles, probably due to the joints between adjacent plates of plexiglas forming the flume walls, the roughness height of the wall was estimated at k_s = 0.02 mm. In the second series of tests, a layer of uniform stones of about 8 mm, respectively 15 mm in diameter was placed on the bottom of the flume. The roughness height was considered equal to the stone diameter, and validated by the comparison between measured and computed water surface profiles (figure 4), at least in the lower range of consider discharges. For higher discharges, waves in the flume lead to a higher variability of the measurement water levels.

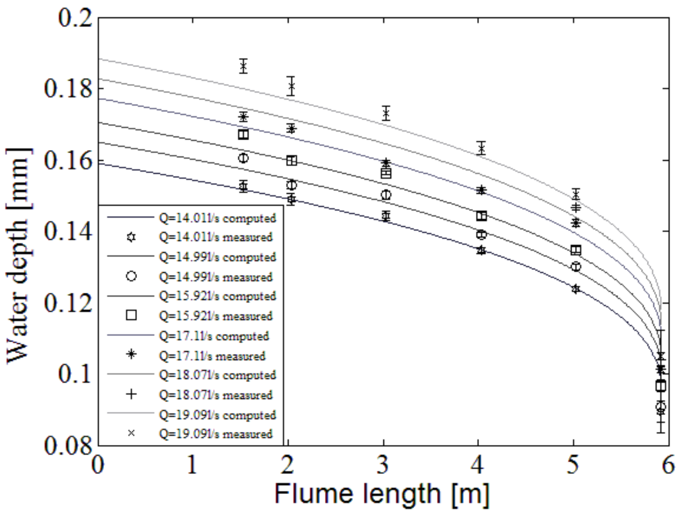

Figure 4 Comparison between computed water surface profile and the measured values, with roughness factor of k_s (wall) = 0.00002 m and k_s (bottom) = 0.015 m

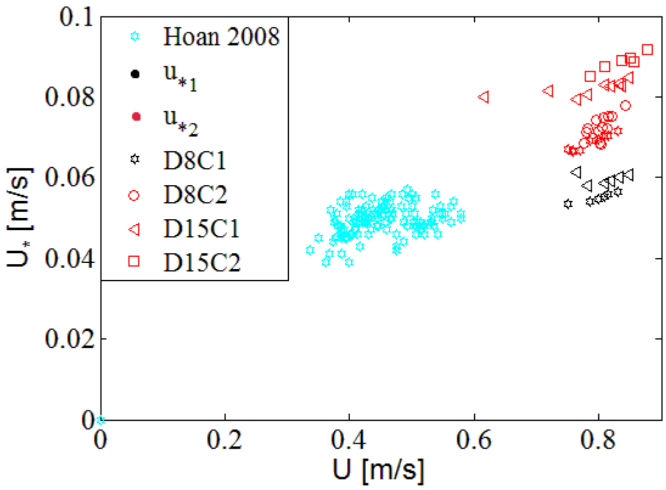

Figure 5. Computed shear velocity with eq. 2 and eq. 3

The shear velocity was deduced from equation 2 and the obtained values are presented in figure 5.

$$\frac{u_{*1}}{u} = \sqrt{\frac{f}{8}} \qquad (2)$$

where f = friction coefficient which takes into consideration the flow friction with the PVC walls and with the flume bed obtained with Barr-Bathurst formula (Machiels et al. 2011).

Another method to compute the shear velocity is by fitting a logarithmic law to the measured velocity profiles:

$$\frac{u}{u_{*2}} = \frac{1}{\kappa}\ln(30\frac{z}{k_s}) \qquad (3)$$

In figure 5 it can be seen the difference between the values of shear velocity obtained by two equations, which highlight the importance of choosing the proper one, especially for further computation, as stones stability assessment.

Equation (3) is strictly valid only over the logarithmic layer in the flow depth. Figure 6 sketches the different layers of an open channel flow over a rough bed. The actual velocity profile deviates from the logarithmic profile near the rough bottom, due to the existence of a roughness layer where the sediments protrude from the bed, as well as in the outer region. So the logarithmic layer remains valid, near the riverbed, in the case of fully turbulent flow, until the level of 0.2h according to (Monin and Yaglom 1971) or (Nezu and Nakagawa 1993); 0.25h (Bagherimiyab and Lemmin 2013) or 0.5h according to (Smart 1999).

In the present experiments, the bed level is considered as the flume bottom due to the presence of a single layer of stones. The virtual bed level is defined as the location where a time-averaged velocity profile predicts u = 0 when extrapolated down into the bed roughness region. The virtual bed level is noted Z_0 level. According to De Bruin and Moore (1985), Z_0 = D/3.85, where D is the displacement of bed level below the top of the roughness elements, in this case the diameter of the stones. Flow depth *h* and the level of velocity measurements are taken regarding the Z_0 position.

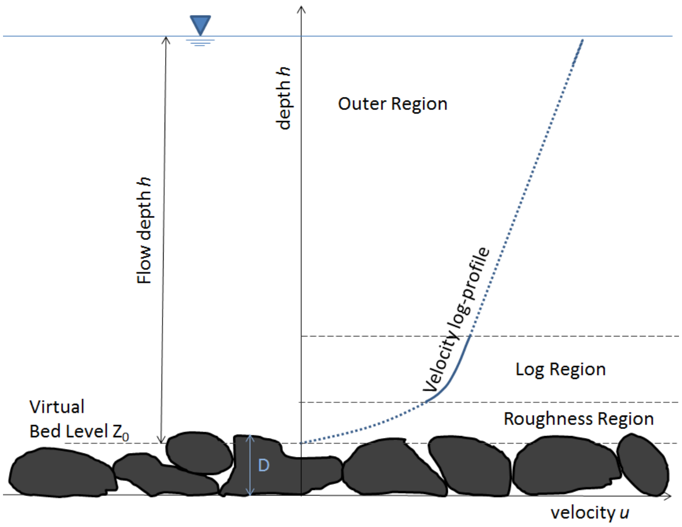

Figure 6. Layers of an open channel flow over a rough bed

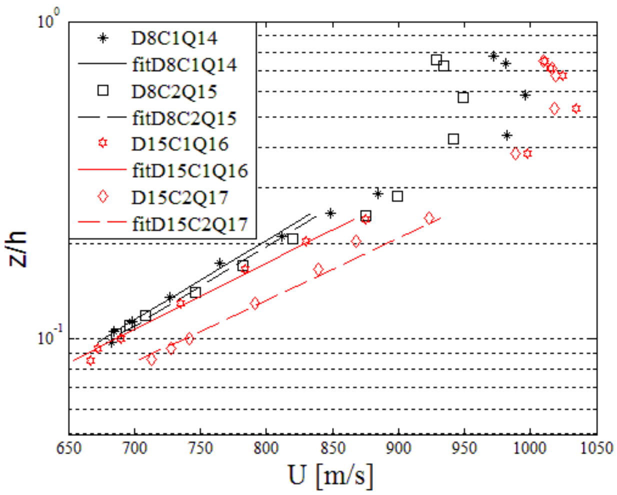

Figure 7. Fit of eq. 3 with the measurements for diameter 8 mm (D8), respectively 15 mm (D15), both configuration (C1 and C2), discharge between 14 l/s and 17 l/s

Representative profiles are given in logarithmic form (Figure 7). The plain and dashed lines represent fitting of equation (3). The fitted lines closely follow the recorded values of velocity. Due to the size of the UVP instrument, no measurements were available very close to the bed, to check the deviation of the velocity profile from its logarithmic form. The lowest point were the velocity was measured, located at about 7 to 9 % from the total flow depth, belongs to logarithmic layer of the flow as it can be seen in Figure 7. The logarithmic profile was fitted for each profile and the regression coefficient was computed. A loop was started from the lowest point and consecutively included the next higher data point. For the best R^2 obtained, the superior limit of logarithmic layer and the shear velocity were retained. The best fit was reached for *z/h*=0.2 (figure 7). This limit is consistent with the conclusions of Bagherimiyab and Lemmin (2013).

4.3. Turbulent kinetic energy

In turbulent flows, the instantaneous velocities *u*, *v* and *w* fluctuate in direction and intensity, around a mean value ($u_i = \bar{u} + u'$). The fluctuating components *u'*, *v'* and *w'* are generally weaker than the mean flow velocity.

The depth averaged turbulent kinetic energy is

$$\mathrm{k_0} = \frac{1}{\mathrm{h}}\int_0^{\mathrm{h}} \mathrm{k(z)dz} \qquad (4)$$

with $\mathrm{k(z)} = \frac{1}{2}(\overline{\mathrm{u'^2}} + \overline{\mathrm{v'^2}} + \overline{\mathrm{w'^2}}),\quad \mathrm{u'(i) = u(i)} - \bar{\mathrm{u}}$ the longitudinal velocity fluctuation, $\overline{\mathrm{v'^2}} = 0.5041\overline{\mathrm{u'^2}}$ and $\overline{\mathrm{w'^2}} = 0.3025\overline{\mathrm{u'^2}}$ the mean squared values of fluctuation in vertical, respectively transversal direction.

The two latest above formulae were developed for smooth flow conditions by Nezu and Nakagawa (1993). Here, measurements in the longitudinal and the vertical directions were performed. Constants of 0.3181, for smooth bed, and 0.3147, for rough bed, were obtained to compute the mean of the square of the vertical velocity fluctuation. Therefore, Nezu's formulae where considered as reasonable approximations for the computation of turbulent kinetic energy.

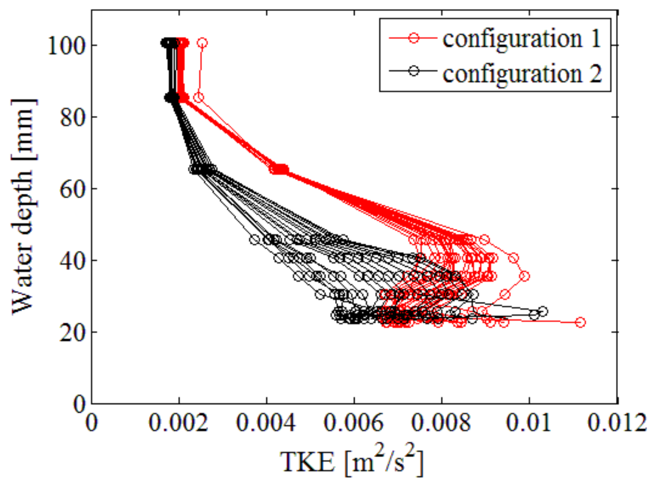

Figure 8. TKE profile along X-axis in a flow of Q=16 l/s, over sediments of 15 mm diameter)

Although the flow is quasi uniform in terms of mean velocity profiles, figure 8 reveals that the lower part (near-bed) of the profiles of turbulent kinetic energy (TKE) varies in the longitudinal direction. In configuration 1, where the flow is expected to be uniform, this suggests that the length of the experimental flume is not sufficient for the TKE profiles to be completely developed. In a later stage of this research, the use of a larger-scale facility, with a length exceeding three times the present one, will enable to investigate fully developed turbulent flow conditions.

Figure 9 shows the difference among turbulent kinetic energy profiles developed in flows of the same mean velocity, but different configurations of the bed.

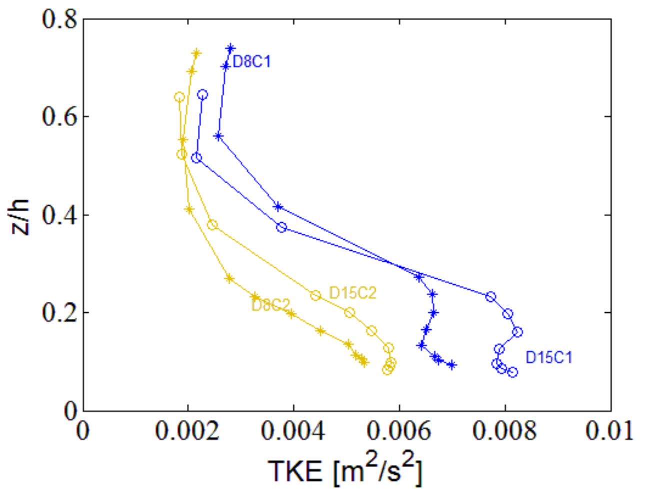

Figure 9. TKE profiles over a rough bed, respectively transition smooth-to-rough, (d=8 mm and d=15 mm), for a discharge of 16 l/s.

4.4. *Stability parameter*

Shields (1936) assumed that the factor in determining the stability of the particles is the ratio of the load on the particle to the strength of the particle (the gravitational force that resists to stone motion):

$$\Psi_S = \frac{\text{load}}{\text{strength}} = \frac{u_*^2}{\Delta g d} \tag{5}$$

So the Shields stability parameter does not consider directly the turbulence of the flow. It is accounted for only indirectly through the friction formulas developed only for uniform flows.

Other formulas exist in the literature for the stability parameter, which consider explicitly the turbulence in their formulation. (Hofland 2005, Hoan 2008, Jongeling et al. 2003) developed a method designed to use the outputs of detailed numerical flow computations for determining damage of bed protections. A combination of velocity and turbulence distributions over a certain water column above the bed is used to quantify the flow forces. The turbulence is incorporated to account for the peak values of the forces that occur in the flow. A Shields-like stability parameter was proposed by each of them:

$$\Psi_{WL} = \frac{\langle(\bar{u}+\alpha\sqrt{k})^2\rangle_{hm}}{\Delta g d} \quad \text{(Jongeling et al. 2003)} \tag{6}$$

$$\Psi_{Lm} = \frac{\max\left[\langle\bar{u}+\alpha\sqrt{k}\rangle_{Lm}\frac{Lm}{z}\right]^2}{\Delta g d} \quad \text{(Hofland 2005)} \tag{7}$$

$$\Psi_{u-\sigma[u]} = \frac{\langle[\bar{u}+\alpha\sigma(u)]^2\sqrt{1-z/h}\rangle_h}{\Delta g d} \quad \text{(Hoan 2008)} \tag{8}$$

where k denotes the turbulent kinetic energy, α is an empirical turbulence magnification factor, $\langle\ldots\rangle_{hm}$ is a spatial average over a distance of hm above the bed. *Lm* denotes the Bakhmetev mixing length ($Lm = \kappa z\sqrt{1-z/h}$), $\langle\ldots\rangle_{Lm}$ is a moving average with varying filter length *Lm*, and *z* is the distance from the bed. The determination of α and *hm* for the new stability Ψ_{WL} and its critical value $\Psi_{WL,c}$ is based on the stability threshold concept.

Hoffmans (2012) adopted the Shields formula using directly the turbulent kinetic energy. He noted $r_0 = \frac{\sqrt{k_0}}{U_0} = 1.2\,\frac{u_*}{U_0}$ for uniform flow, so he obtained $u_* = \frac{r_0 U_0}{1.2}$ and $\tau_c = \Psi_S(\rho_s - \rho)gd$ as Shields critical parameter developed for uniform flows and low slopes.

Finally, he noted with d_n = 0.84 d and obtained:

$$d_n = 0.84 * 0.6944 * \frac{(r_0 U_0)^2}{\Psi_c \Delta g} \tag{9}$$

He reports experimental tests involving non-uniform flows for which he applied both formulas (eq. 5 and eq. 9). The Shields formula does not lead to a satisfactory correlation with the inception of sediment motion. In contrast Hoffmans' formula, by measuring directly the turbulent kinetic energy, predicted much more consistent results.

4.5. *Mobility parameter*

A clearly defined and quantified measure of damage is essential for assessing the stability of a granular bed. This quantity is often referred to as mobility parameter (or bed damage indicator). This parameter should adequately quantify the bed response (also the bed damage level) for a variety of flow conditions, including uniform and non-uniform.

In this work, a series of experimental tests were performed to collect data over the number of stones entrained under given flow conditions. Over a uniform riverbed (configuration 1), with sediments of 8 mm, respectively 15 mm, a flow of discharge between 13 l/s and 18 l/s was run continuously for 2*h*.

The mobility of stones is defined as the number of pick-ups per unit of time (T) and area (A):

$$E = \frac{nd^3}{AT} \tag{10}$$

$$\phi = \frac{E}{\sqrt{\Delta g d}} \tag{11}$$

where E is the entertainment rate, n is number of displaced stones, ϕ_E is the mobility parameter, Δ is the specific submerge density and d is the characteristic particle diameter. The results are presented in figure 10(a-d).

Figure 10 shows the results obtained in the present study, when the five formulae (eq. 5 to 9) mentioned previously are applied. The new results are compared with the data of Hoan (2008) (fig. 10 (a - d)). Using the Shields parameter leads to a high scatter of experimental data (figure 10(a)).

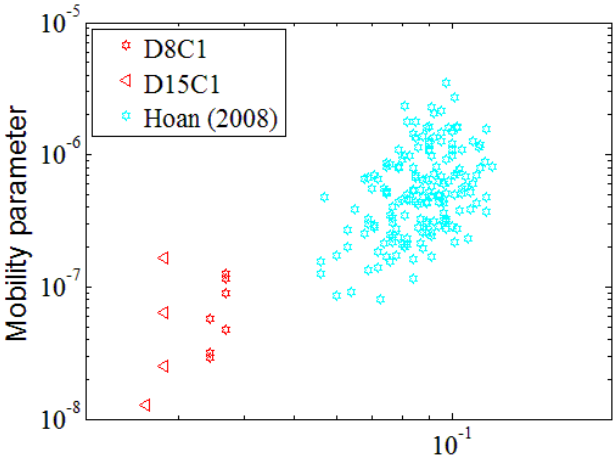

$$\Psi_S = \frac{\text{load}}{\text{strength}} = \frac{u_*^2}{\Delta gd} \text{ (Shields 1936)}$$

Figure 10a. Measured Ψ_S versus measured ϕ

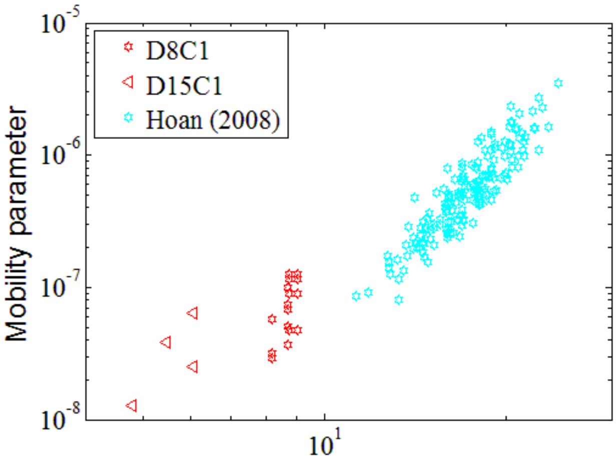

$$\Psi_{WL} = \frac{\langle(\bar{u}+\alpha\sqrt{k})^2\rangle_{hm}}{\Delta gd} \text{ (Jongeling et al. 2003)}$$

Figure 10b. Measured Ψ_{WL} versus measured ϕ

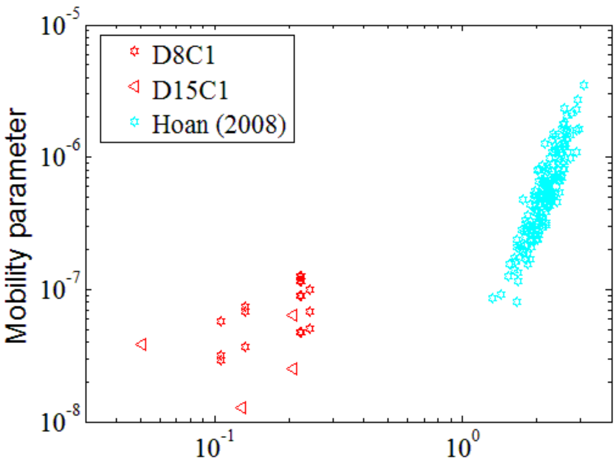

$$\Psi_{Lm} = \frac{\max\left[\langle\bar{u}+\alpha\sqrt{k}\rangle_{Lm}\frac{Lm}{z}\right]^2}{\Delta gd} \text{ (Hofland 2005)}$$

Figure 10c. Measured Ψ_{Lm} versus measured ϕ

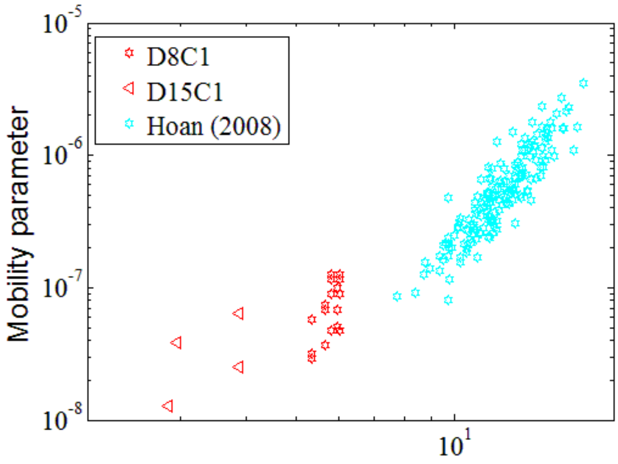

$$\Psi_{u-\sigma[u]} = \frac{\langle[\bar{u}+\alpha\sigma(u)]^2\sqrt{1-z/h}\rangle_h}{\Delta gd} \text{ (Hoan 2008)}$$

Figure 10d. Measured $\Psi_{u-\sigma[u]}$ versus measured ϕ

The parameter introduced by Jongeling et al. (2003), Hofland (2005) and Hoan (2008) lead to more consistent results (figure 10(b-d)), as turbulence is taken into consideration more explicitly. As shown in figure 10(b-d), the new results extend the range of investigated stability and mobility parameters to lower values than previously available. The new results show also a mostly consistent trend compared to data by Hoan (2008).

5. DISCUSSION AND CONCLUSION

The two configurations used in the experimental procedure showed that over a rough boundary, friction created by gravel particles retards the flow velocity and increase the turbulence intensity, but the effect diminishes with increasing height above the bed (Jay Lacey and Roy 2008, Lacey and Roy 2007). Due to these flow structures, developed by the roughness elements, the variation of lift and drag forces increase and so the entrainment of particles is more likely to appear (Schmeeckle et al. 2007, Hardy et al. 2009). This idea is sustained by the present work, where for the same mean velocity and hydraulic conditions, but different turbulent structures, the results regarding the inception of motion are different.

Two configurations were considered, a uniform rough river bed and transition from smooth to rough. The flow characteristics were studied by measuring the velocity profile in the main direction of the stream with a UVP transducer. The shear velocity was computed with two methods, by friction formulas and by fitting a logarithmic equation. The turbulent kinetic energy profiles were developed and compared. In a second series of tests, the movement of the stones was observed. The threshold of inception of motion was recorded and then data over the quantity of displaced sediments was collected. Finally different equations for assessing the stability of riverbeds were applied on the present experiments and compared with other results from literature. Although the standard Shields method is largely used, this work highlights its shortcomings. The flow turbulence is an important parameter which has to be explicitly taken into consideration especially in case of non-uniform flows. In addition, the entertainment rate concept offers a better view regarding the stability of protection layer than the threshold concept.

6. REFERENCES

Bagherimiyab, F. and U. Lemmin (2013). "Shear velocity estimates in rough-bed open-channel flow." Earth Surface Processes and Landforms: 38: 1714-1724.

Buffington, J. M. and D. R. Montgomery (1997). "A systematic analysis of eight decades of incipient motion studies, with special reference to gravel-bedded rivers." Water Resources Research 33(8): 1993-2029.

Cataño-Lopera, Y. A., B. J. Landry, J. D. Abad and M. H. García (2013). "Experimental and Numerical Study of the Flow Structure around Two Partially Buried Objects on a Deformed Bed." Journal of Hydraulic Engineering 139(3): 269-283.

De Bruin, H. A. R. and C. J. Moore (1985). "Zero-plane displacement and roughness length for tall vegetation, derived from a simple mass conservation hypothesis." Boundary-Layer Meteorology 31(1): 39-49.

Dwivedi, A., B. Melville, A. J. Raudkivi, A. Y. Shamseldin and Y.-M. Chiew (2012). "Role of Turbulence and Particle Exposure on Entrainment of Large Spherical Particles in Flows with Low Relative Submergence." Journal of Hydraulic Engineering 138(12): 1022-1030.

Fukuoka, S. (2013). Prediction of three-dimensional movement of gravel particles in a movable-bed numerical channel. THESIS. Chatou France.

Goring, D. and V. Nikora (2002). "Despiking Acoustic Doppler Velocimeter Data." Journal of Hydraulic Engineering 128(1): 117-126.

Hardy, R. J., J. L. Best, S. N. Lane and P. E. Carbonneau (2009). "Coherent flow structures in a depth-limited flow over a gravel surface: The role of near-bed turbulence and influence of Reynolds number." Journal of Geophysical Research: Earth Surface (2003–2012) 114(F1).

Hoan, N. T. (2008). Stone Stability Under Non-uniform Flow, Delft Univ. of Technology.

Hoffmans, G. J. C. M. (2012). The Influence of Turbulence on Soil Erosion. Delft, The Netherlands, Eburon Uitgeverij B.V.

Hofland, B. (2005). Rock and roll: turbulence-induced damage to granular bed protections, Delft Univ. of Technology.

Jay Lacey, R. W. and A. G. Roy (2008). "Fine-scale characterization of the turbulent shear layer of an instream pebble cluster." Journal of Hydraulic Engineering 134(7): 925-936.

Jeffcoate, P., P. Stansby and D. Apsley (2012). "Flow Due to Multiple Jets Downstream of a Barrage: Experiments, 3-D CFD and Depth-Averaged Modelling." Journal of Hydraulic Engineering 139(7): 754-762.

Jongeling, T. H. G., A. Blom, H. R. A. Jagers, C. Stolker and H. J. Verheij (2003). Design method granular protections.Technical Rep. Q 2933. Delft, The Netherlands, Delft University of technology.

Lacey, R. W. and A. G. Roy (2007). "A comparative study of the turbulent flow field with and without a pebble cluster in a gravel bed river." Water Resources Research 43(5).

Machiels, O., S. Erpicum, P. Archambeau, B. Dewals and M. Pirotton (2011). "Theoretical and numerical analysis of the influence of the bottom friction formulation in free surface flow modelling." Water SA 37(2).

Met-Flow, S. A. (2000). "UVP monitor—User’s guide." Lausanne, Switzerland.

Nezu, I. and D. Kyōto (1977). Turbulent structure in open-channel flows, Dept. of Civil Engineering, Kyoto University.

Nezu, I. and H. Nakagawa (1993). Turbulence in open-channel flows. Rotterdam, A.A. Balkema.

Schmeeckle, M. W., J. M. Nelson and R. L. Shreve (2007). "Forces on stationary particles in near-bed turbulent flows." Journal of Geophysical Research: Earth Surface (2003–2012) 112(F2).

Shields, A. (1936). Anwendung der Ahnlichkeitsmechnik und der Turbulenz Forscung auf die Geschiebebewegung (Application of similarity principles and turbulence research to bed-load movement). Mitt. der Preuss. Versuchsamst. fur Wasserbau und Schiffbau., Heft 26, Berlin, Germany.

Smart, G. (1999). "Turbulent Velocity Profiles and Boundary Shear in Gravel Bed Rivers." Journal of Hydraulic Engineering 125(2): 106-116.

Yalin, M. S. (1977). Mechanics of sediment transport, Pergamon, New York.